Journal of Pathology
J Pathol 2019; **248:** 488–500
Published online 7 May 2019 in Wiley Online Library (wileyonlinelibrary.com) DOI: 10.1002/path.5275

ORIGINAL PAPER

Bone marrow-derived macrophage contributes to fibrosing steatohepatitis through activating hepatic stellate cells

Juqiang Han[1,2†], Xiang Zhang[1†], Jennie K-C Lau[3], Kaili Fu[1], Harry CH Lau[1], Weiqi Xu[1], Eagle SH Chu[1], Huiyao Lan[4] and Jun Yu[1*]

[1] *Institute of Digestive Disease, Department of Medicine and Therapeutics, State Key Laboratory of Digestive Disease, Li Ka Shing Institute of Health Sciences, CUHK Shenzhen Research Institute, The Chinese University of Hong Kong, Hong Kong SAR*
[2] *Institute of Liver Disease, The Seventh Medical Centre of PLA General Hospital, Beijing, PR China*
[3] *Faculty of Medicine, SHHO College, The Chinese University of Hong Kong, Hong Kong SAR*
[4] *Department of Anatomical and Cellular Pathology, Li Ka Shing Institute of Health Sciences, Department of Medicine & Therapeutics, The Chinese University of Hong Kong, Hong Kong SAR*

**Correspondence to: J Yu, Institute of Digestive Disease, Department of Medicine and Therapeutics, Prince of Wales Hospital, The Chinese University of Hong Kong, Shatin, NT, Hong Kong SAR. E-mail: junyu@cuhk.edu.hk*

†These authors contributed equally to this work.

Abstract

The role of macrophages in fibrosing steatohepatitis is largely unclear. We characterized the origin and molecular mechanisms of macrophages and its targeted therapy of fibrosing steatohepatitis. Fibrosing steatohepatitis was established in Alms1 mutant (*foz/foz*) and C57BL/6J wildtype mice fed high-fat/high-cholesterol or methionine- and choline-deficient diet. Bone marrow transplantation was performed to track the macrophage origin in fibrosing steatohepatitis. Macrophages were depleted using liposomal clodronate. Primary macrophages were isolated from bone marrow for adoptive transfer into mice. We found that macrophage infiltration is induced in two mouse models of fibrosing steatohepatitis and human nonalcoholic steatohepatitis-fibrosis patients. Bone marrow-derived macrophages (BMMs) contribute to the hepatic macrophage accumulation in experimental fibrosing steatohepatitis. Depletion of hepatic BMMs by liposomal clodronate during liver injury attenuated fibrosing steatohepatitis, whilst BMMs depletion after liver injury delayed the regression of fibrosing steatohepatitis. The pro-fibrotic effect of macrophages was associated with reduced activation of hepatic stellate cells (HSCs), collagen deposition and hepatic expression of key pro-fibrotic factors (TIMP1, TIMP2, and TGFβ1) and endoplasmic reticulum stress markers (GRP78, IRE1α, and PDI). Conversely, adoptive transfer of BMMs significantly aggravated fibrosing steatohepatitis. Moreover, macrophage-conditioned medium directly promoted the phenotypic transition of primary quiescent HSCs to activated HSCs; it enhanced activation and proliferation but decreased apoptosis of HSC cell lines (LX-2 and HSC-T6). The effect of BMMs in promoting fibrosing steatohepatitis was mediated by inducing key pro-fibrosis factors and signaling pathways including cytokine/chemokine, TGFβ and complement cascade as assessed by cDNA expression array. Complement 3a receptor (C3ar1) was a predominant effector of macrophage mediated fibrosing steatohepatitis. Knockout of *C3ar1* in mice blunted development of fibrosing steatohepatitis. In conclusion, BMMs promoted the progression of fibrosing steatohepatitis during injury, whereas macrophages reduced fibrosing steatohepatitis in the recovery phase of liver injury. Increasing anti-fibrotic macrophages and decreasing pro-fibrotic macrophages are promising approaches for fibrosing steatohepatitis.

Keywords: bone marrow-derived monocytes; nutritional fibrosis; hepatic stellate cells; C3ar1; target therapy

Received 9 August 2018; Revised 26 February 2019; Accepted 28 March 2019

No conflicts of interest were declared.

Introduction

Nonalcoholic steatohepatitis (NASH) has a worldwide distribution that parallels the rapid increase in the incidence of obesity. NASH can progress through stages of fibrosis, cirrhosis, and eventually to end-stage liver failure. Cirrhosis has been predicted to become the most common indication for liver transplantation [1]. Despite the extensive literature on NASH, the pathogenesis of NASH-related fibrosis (fibrosing steatohepatitis) still remains obscure and numerous clinical cases of advanced cirrhosis are still largely irreversible [2]. There is thus compelling need to identify new promising anti-fibrotic targets.

Development of fibrosing steatohepatitis is a complex process that involves multicellular responses with activation of hepatic stellate cells (HSCs). The immune system can regulate both the progression and regression of the fibrotic process. Anti-fibrotic strategies are emerging that manipulate the immune system in

experimental systems [3]. Among the immune cell populations, macrophages are considered the first line of defense against hepatocyte injuries, and a key player in the fibrotic cascade [4]. Macrophages can exist in tissues as tissue-resident macrophages (e.g. Kupffer cells in the liver), but can also arise from blood monocytes originating in the bone marrow, to yield bone marrow-derived macrophages (BMMs) [5]. It has been reported that macrophages constitute an essential component for the process of fibrosis through secretion of pro-fibrogenic cytokines [4]. However, the mechanism of action and origin of macrophages in fibrosing steatohepatitis are unexplored. More importantly, there is no evidence available on whether macrophages can be targeted for the treatment of fibrosing steatohepatitis.

In this study, we aimed to characterize the origin and molecular regulators of macrophages, and assess the therapeutic potential of macrophage-targeted therapy against fibrosing steatohepatitis. First, we identified the macrophages that infiltrate the liver tissues of two mice models of fibrosing steatohepatitis and human NASH-fibrosis patients. Subsequently, using bone marrow transplantation (BMT), we demonstrated that BMMs is the predominant population contributing to the enhanced macrophage infiltration in fibrosing steatohepatitis. Drug intervention was then used to deplete BMMs in both dietary and genetic fibrosing steatohepatitis models. Our results showed that BMMs have a pro-fibrogenic role during the injury. In contrast, macrophages possess anti-fibrotic activity during the recovery. Additionally, adoptive transfer of BMMs in mice further confirmed the essential role of BMMs in inducing fibrosing steatohepatitis. Mechanistically, BMMs-induced fibrosing steatohepatitis was mediated by inducing hepatic Complement 3a receptor 1 (C3ar1) and consequent HSC activation.

Materials and methods

Mouse models of fibrosing steatohepatitis

Fibrosing steatohepatitis was induced in male C57BL/6J mice (age 8 weeks) by feeding them a methionine- and choline-deficient (MCD) diet for 8 weeks [6]. Control mice were fed with MCD control diet (ICN Biomedical, Costa Mesa, CA, USA). In a second mouse model of fibrosing steatohepatitis, male Alms mutant (*foz/foz* mice) (age 8 weeks) were fed a high-fat/high-cholesterol (HFHC) diet (Specialty Feeds, Glen Forrest, WA, Australia) for 12 weeks [7]. The *foz/foz* control mice were fed control diet. Male *C3ar1* knockout ($C3ar1^{-/-}$) mice (age 8 weeks) (kindly provided by Professor Jie Du, Key Laboratory of Remodeling-related Cardiovascular Diseases, Capital Medical University, P.R. China) were fed a MCD or control diet for 8 weeks. Transgenic lysM-Cre/DTR mice were challenged with MCD or control diet for 5 weeks. The number of mice per group was 5–8. All animal studies were performed in accordance with guidelines approved by the Animal Experimentation Ethics Committee of the Chinese University of Hong Kong and Capital Medical University.

Human samples

Human liver tissues were obtained from 28 subjects (10 NASH-fibrosis patients and 18 normal subjects) from percutaneous liver biopsy specimens (see supplementary material, Tables S1 and S2). The normal liver tissues were obtained from the donors of liver transplantation in Queen Mary Hospital, the University of Hong Kong. The main reasons for liver biopsy in NASH-fibrosis patients were abnormal liver function tests and/or abnormal imaging results. Patients with history of excessive alcohol consumption (more than 30 g/day for men and 20 g/day for women), secondary causes of hepatic steatosis, positive hepatitis B surface antigen, anti-hepatitis C virus antibody, or histological evidence of other concomitant chronic liver diseases were excluded [8]. The liver histology of these NASH-fibrosis patients was examined by two experienced pathologists. The overall NASH diagnosis is according to the EASL-EASD-EASO Clinical Practice Guidelines on NAFLD [9] and Practice Guidance by the American Association for the Study of Liver Diseases [10]. NASH was diagnosed for specimens with macrovesicular steatosis, hepatocellular ballooning, and lobular inflammatory infiltrates. Liver histology was reported by semiquantitative scoring of four histological features including steatosis (0–3), lobular inflammation (0–3), hepatocellular ballooning (0–2), and fibrosis (0–4). NAFLD activity score was the sum of steatosis, lobular inflammation, and hepatocellular ballooning scores. Control subjects had normal liver histology or less than 5% of hepatic triglyceride content measured by proton-magnetic resonance spectroscopy with no history of diabetes or hypertension. All subjects were given written informed consent prior to sample collection and the study protocol was approved by the Clinical Research Ethics Committee of the Chinese University of Hong Kong and the University of Hong Kong.

Liver specific macrophage depletion during liver injury and recovery

Macrophage depletion during liver injury was achieved by intraperitoneal injection of liposomal clodronate (5 mg/ml, 100 µl per 10 g mouse; Liposoma, Amsterdam, The Netherlands) twice, at week 7 and week 8 separately in WT mice fed MCD, and at week 11 and week 12 in *foz/foz* mice [11].

For macrophage depletion during recovery from fibrosis, male C57BL/6J mice were fed with MCD diet for 8 weeks, then changed to control diet at week 9. Liposomal clodronate or control liposomes were injected intraperitoneally twice during week 9. Livers were harvested 2 days after the final dose of liposomal clodronate or control liposomes.

Isolation of BMMs

Bone marrow cells were isolated from the femur and tibia of 8-week-old male C57BL/6J mice. To obtain macrophage colony stimulating factor from fibroblast conditioned medium (FCM), L929 fibroblasts were cultured in RPMI 1640 medium (Thermo Fisher, Waltham, MA, USA) with 10% FBS for 3 days and the supernatant FCM was collected and centrifuged at 12 000 × *g* for 10 min. The centrifuged FCM was stored at −80 °C. Bone marrow cells were cultured in DMEM medium (Thermo Fisher) containing 10% FBS and 20% FCM for 1 week [12] to generate BMMs. By the 7th day, all adherent cells had become mature macrophages [13]. The F4/80$^+$ BMMs population was then purified by flow cytometry assay (>99% purity).

cDNA expression array analyses

Gene expression array of liver tissues was analyzed by the Mouse Inflammatory Response & Autoimmunity PCR Array (SABiosciences, Frederick, MD, USA). The array system can detect 84 key genes involved in autoimmune and inflammatory immune responses (http://www.sabiosciences.com). Gene expression with fold-changes ≥1.5 was considered to be of biological significance. PCR array data are provided as supplementary material, Appendix 1.

Detailed methods for BMT, histopathology, biochemical assays and inflammatory cytokine profiling assays, adoptive macrophage transfer of bone marrow cells, isolation and culture of mouse primary HSCs, co-culture of macrophages and HSCs, cell growth and apoptosis assays, western blotting, immunofluorescence, RT-qPCR, and immunohistochemistry are provided in supplementary information, Supplementary materials and methods.

Statistical analyses

The Shapiro–Wilk test was performed to assess if the data plausibly came from a normal distribution. Differences between the two groups were assessed by Student's *t*-test or nonparametric Mann–Whitney test. Multiple group comparisons were made using one-way ANOVA or a Kruskal–Wallis test (GraphPad Inc, San Diego, CA, USA). Spearman's rank-sum correlation analysis was performed to determine the co-expression pattern. Data were expressed as mean ± SD and considered significant if $p < 0.05$.

Results

Macrophage infiltration was significantly induced in fibrosing steatohepatitis of mouse models and human patients

First, we evaluated macrophage infiltration in HFHC diet-induced *foz/foz* mouse models and MCD diet-induced C57BL/6J mouse models of fibrosing steatohepatitis. *foz/foz* mice fed a HFHC diet for 12 weeks and C57BL/6J mice fed a MCD diet for 8 weeks developed fibrosing steatohepatitis, indicated by increased collagen deposition assessed by Picro-Sirius Red staining and increased lipid accumulation and inflammatory cell infiltration demonstrated by H&E staining (Figure 1A,B). Concomitantly, mice macrophage marker F4/80 was significantly upregulated in fibrosing steatohepatitis in both animal models ($p < 0.001$, Figure 1A,B). Co-immunofluorescence of F4/80 and alpha-smooth muscle actin (α-SMA) showed that macrophages and HSCs were not co-localized in the liver tissues of fibrosing steatohepatitis (Figure 1B), thus HSCs in liver fibrogenesis were not derived from macrophages.

We validated the hepatic levels of macrophages by examining CD68 (a macrophage-specific marker) in human liver tissues of 10 NASH-related fibrosis and 18 normal controls. *CD68* mRNA expression was significantly higher in human NASH-related fibrosis compared with normal controls as determined by RT-qPCR (2.58 ± 0.88 versus 1.01 ± 0.38, $p < 0.001$) (Figure 1C). *CD68* mRNA expression was found to be positively associated with the levels of mRNA encoding the HSC activation marker α-SMA in human samples from NASH-fibrosis and control subjects ($r = 0.50$, $p < 0.01$, Figure 1C). The upregulated CD68 protein levels in human NASH-fibrosis tissues and the association of macrophage and fibrosis were further confirmed by co-immunohistochemistry of CD68 and α-SMA in human liver tissues of NASH-related fibrosis and normal subjects (Figure 1D). Consistent with the finding in mouse fibrosing steatohepatitis, CD68 and α-SMA were not co-localized in human NASH-fibrotic liver tissues (Figure 1D).

The macrophage accumulation in fibrosing steatohepatitis is originally from bone marrow in mice

BMMs and resident Kupffer cells constitute macrophages in liver. To determine the origin of the increased number of hepatic macrophages in fibrosing steatohepatitis in C57BL/6J mice, we transplanted bone marrow from GFP transgenic (GFP$^+$) mice to C57BL/6J mice by tail vein injection 3 days after sublethal γ-irradiation (Figure 1E). The mice receiving GFP$^+$ bone marrow were fed MCD diet for 8 weeks to induce fibrosing steatohepatitis. All the macrophages in fibrosing steatohepatitis of the recipient mice were GFP$^+$ macrophages as evidenced by co-immunofluorescence for GFP and the macrophage marker F4/80 (Figure 1F), indicating that the increased hepatic macrophages infiltration was of BMMs origin. This finding was confirmed by significantly increased protein expression of Ly6c, a specific BMMs marker, in mice with fibrosing steatohepatitis compared with control mice (Figure 2A).

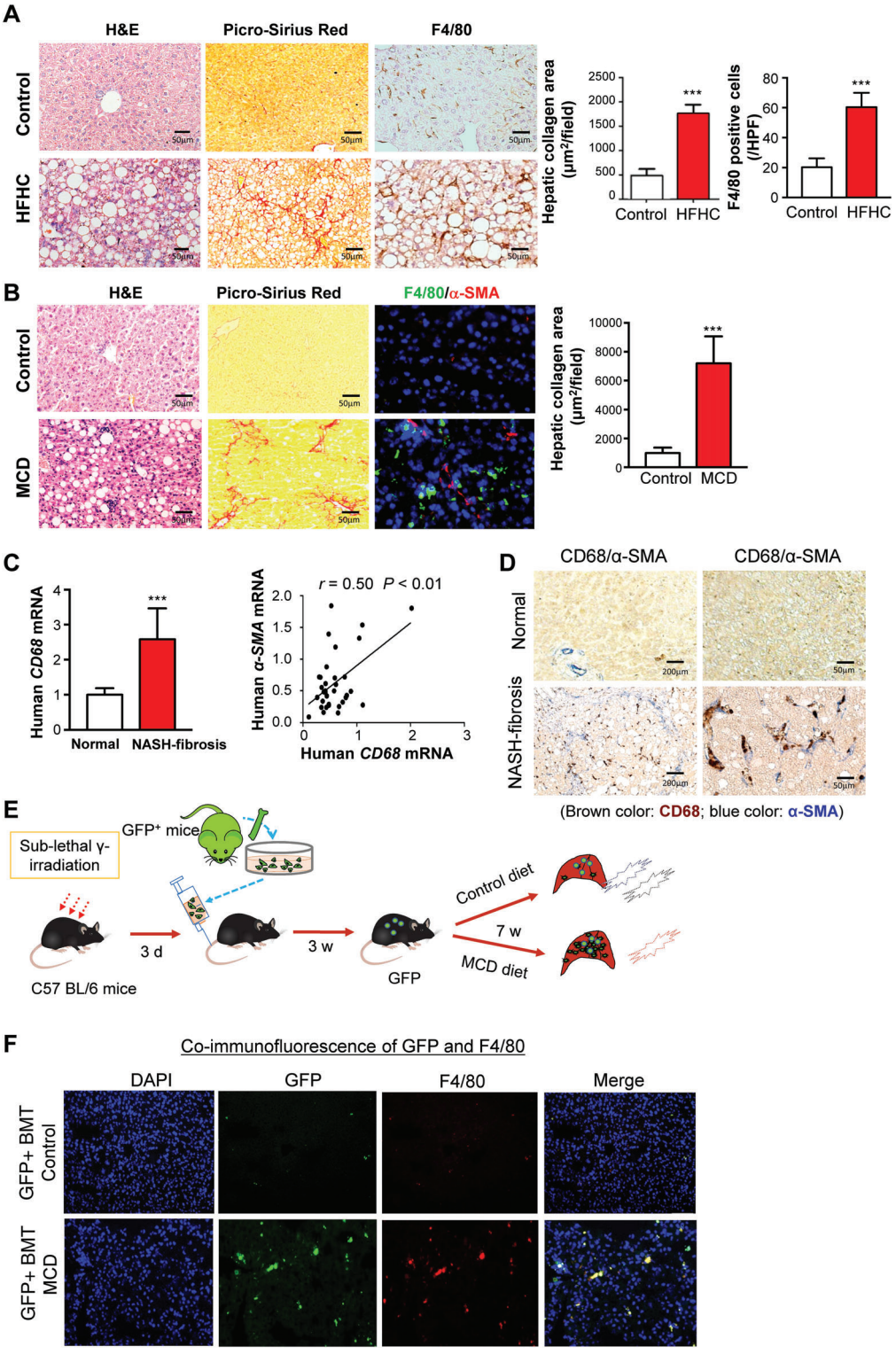

Figure 1. Macrophage infiltration was significantly induced in fibrosing steatohepatitis of two mouse models and human NASH-fibrosis patients, and was attributed to BMMs. (A) Representative H&E staining, Picro-Sirius Red staining and immunohistochemistry for F4/80 in liver tissues from 12 weeks HFHC diet-fed *foz/foz* mice. The amount of collagen protein was determined by Picro-Sirius Red staining. The number of F4/80 positive cells/high-power field was calculated. (B) Representative H&E, Picro-Sirius Red staining, and co-immunofluorescence for F4/80 (green) and α-SMA (red) in liver tissues from 8-weeks MCD diet-fed mice. (C) *CD68* mRNA expression was significantly increased in human NASH-fibrosis liver tissues compared to normal control and positively associated with α-SMA (*ACTA2*) mRNA levels. (D) Representative images of CD68 (brown) and α-SMA (blue) dual-immunostaining of human normal liver tissues and NASH-fibrosis tissues. (E) Schematic diagram of bone marrow transplantation from GFP transgenic mice for determining the origin of macrophages in fibrosing steatohepatitis. (F) Representative immunofluorescence staining of liver tissues from mice transplanted with GFP^+ bone marrow. GFP (green) and F4/80 (red) co-localized on the macrophages in liver tissues from recipient mice fed with MCD diet. $n = 5–8$/group. $^{***}P < 0.001$.

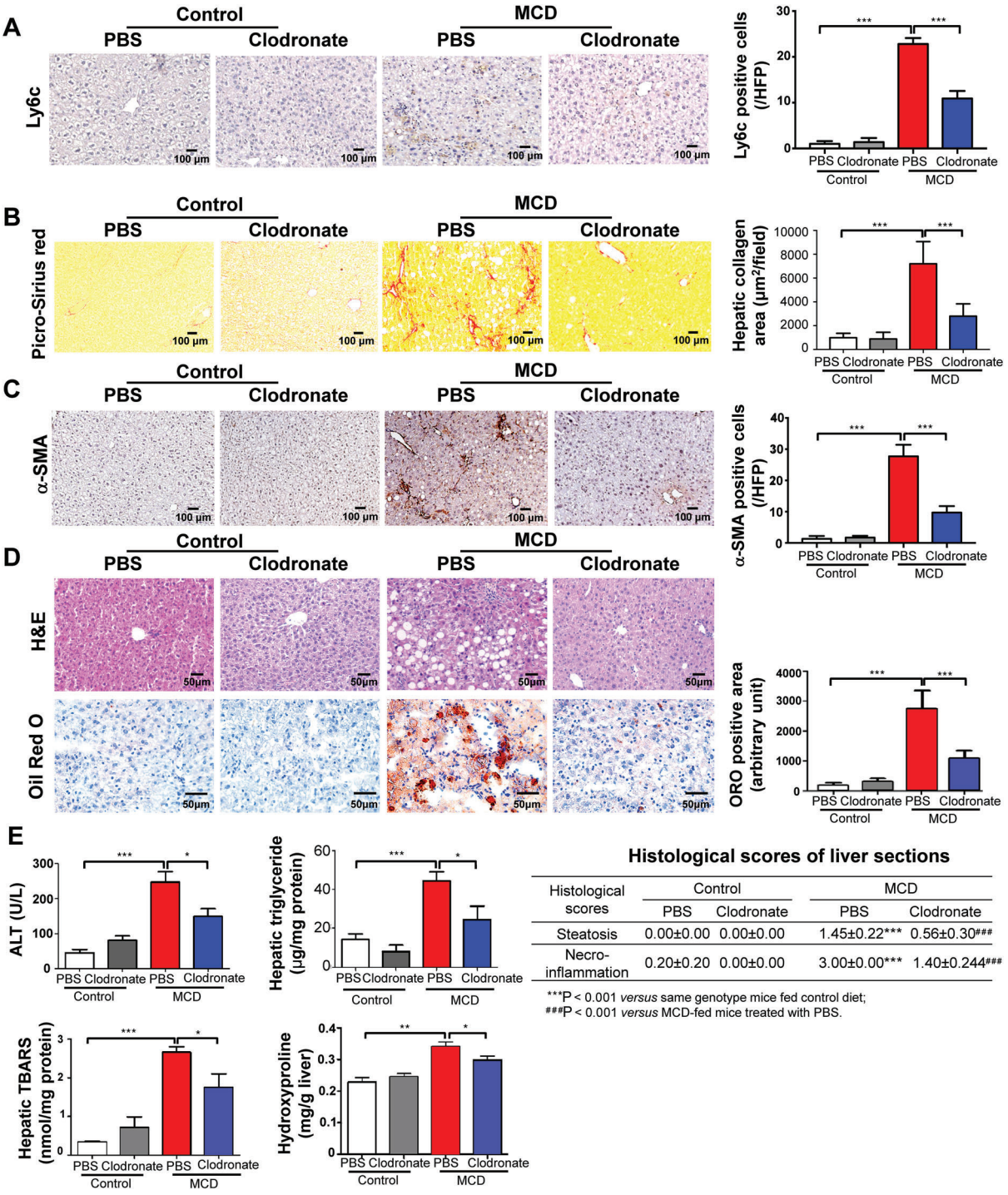

Histological scores of liver sections

Histological scores	Control		MCD	
	PBS	Clodronate	PBS	Clodronate
Steatosis	0.00±0.00	0.00±0.00	1.45±0.22***	0.56±0.30###
Necro-inflammation	0.20±0.20	0.00±0.00	3.00±0.00***	1.40±0.244###

***P < 0.001 *versus* same genotype mice fed control diet;
###P < 0.001 *versus* MCD-fed mice treated with PBS.

Figure 2. Macrophage depletion prevented MCD diet-induced fibrosing steatohepatitis in C57BL/6J mice. (A) Representative immunohistochemistry analysis of Ly6c. (B) Representative Picro-Sirius Red staining of collagen fibers in liver tissues from MCD-fed C57BL/6J mice depleted of macrophages by clodronate treatment. (C) α-SMA protein was analyzed by immunohistochemistry staining. Ten random fields from five slides per group were examined, and α-SMA positive cells were counted (per high-power field). (D) Images of representative H&E and Oil Red O stained liver tissues from 8-weeks MCD-fed C57BL/6J mice depleted of macrophages by clodronate treatment. Histological steatosis and necro-inflammation was scored in liver tissues by H&E staining. Lipid accumulation was shown in liver tissue by Oil Red O staining. (E) Serum ALT, total hepatic lipoperoxide, liver triglyceride content, and hydroxyproline assay were determined. $n = 5–8$/group. $^{*}P < 0.05$, $^{**}P < 0.01$, $^{***}P < 0.001$.

BMMs depletion during injury reduced fibrosing steatohepatitis

To elucidate the role of BMMs in fibrosing steatohepatitis, we depleted macrophages by injecting clodronate-containing liposomes, which could mediate macrophage 'suicide'. Macrophage depletion was achieved by clodronate treatment for 2 weeks in these C57BL/6J mice as evidenced by reduced protein expression of the BMMs marker Ly6C (Figure 2A). Macrophage depletion for 2 weeks in C57BL/6J mice with fibrosing steatohepatitis caused a 61.1% decrease

in collagen fibers (Figure 2B), a 65.0% reduction in α-SMA positive cells (Figure 2C), concomitant with improved liver histology (Figure 2D), and a 59.2% decrease in lipid accumulation (Figure 2D), a 39.2% decrease in ALT levels (Figure 2E), a 34% reduction in hepatic lipid peroxide, a 44.8% decrease in hepatic triglyceride and a 14.7% reduction in hepatic hydroxyproline (Figure 2E). These results further confirmed that BMMs contribute to the development of steatohepatitis and depletion of BMMs protects against the disease progression.

To confirm the effects of BMMs in C57/BL6 mice with fibrosing steatohepatitis, an additional macrophage depletion experiment was performed on *foz/foz* mice fed HFHC diet for 12 weeks with severe fibrosing steatohepatitis (Figure 3A). Clodronate treatment for 2 weeks in these *foz/foz* mice depleted macrophages with reduced protein expression of macrophage marker F4/80 (Figure 3A). As shown in Figure 3A, macrophage depletion ameliorated liver histology with a 65.6% reduced score of hepatic steatosis and a 78.6% reduced score of inflammation, concomitant with a 27.5% reduction in serum ALT, a 12.8% reduction in triglyceride and a 49.3% reduction in hepatic lipid peroxide (Figure 3B). In particular, macrophage depletion significantly blunted the histological severity of fibrosis by 43.3% (Figure 3C), reduced hepatic hydroxyproline content by 38.9% (Figure 3C), decreased the protein expression of collagen I by 80.7%, and α-SMA by 62.7% (Figure 3D,E).

BMMs depletion during recovery from MCD injury led to increased fibrosis

We further determined the effects of macrophages on fibrosing steatohepatitis during the recovery from such injury. Male C57BL/6J mice were fed with MCD diet for 8 weeks to induce fibrosing steatohepatitis. At week 9, mice fed with MCD were changed to control diet to recover the liver injury. Liposomal clodronate was administered twice to deplete macrophages. Macrophage depletion was confirmed by reduced protein expression of F4/80 (see supplementary material, Figure S1A). We found that macrophage depletion during recovery phase of fibrosing steatohepatitis caused levels of collagen fibers to increase by 57.6% (see supplementary material, Figure S1B) and of α-SMA positive cells by 103.1% (see supplementary material, Figure S1C), concomitant with severe liver histology (see supplementary material, Figure S1D), ALT increased by 50.7% (see supplementary material, Figure S1E), and hepatic lipid peroxide by 67.6% (see supplementary material, Figure S1F). These results suggested that macrophage depletion after liver injury aggravated fibrosing steatohepatitis.

BMMs depletion inhibits key pro-fibrosis markers

We examined key fibrosis regulating factors including collagen production (collagen I, TGFβ1), HSC activation (α-SMA) and matrix degradation (tissue inhibitor of metalloproteinase [TIMP]-1, TIMP-2, matrix metalloprotein [MMP]2, MMP9) in fibrosing steatohepatitis with or without macrophage depletion. Macrophage depletion during injury significantly reduced protein expression of collagen I, α-SMA, TIMP-1, TIMP-2, MMP2, MMP9, and TGFβ1 (Figure 3F, see supplementary material, Figure S2), Moreover, the endoplasmic reticulum (ER) stress markers including glucose regulated protein 78 (GRP78), inositol-requiring enzyme1α (IRE1α), and protein disulfide isomerase (PDI) were significantly downregulated by macrophage depletion (Figure 3F, see supplementary material, Figure S2). Hence it is reasonable to infer that the effect of macrophages in promoting fibrosing steatohepatitis was mediated at least partially by inducing pro-fibrotic factors and ER stress.

Adoptive transfer of BMMs aggravated fibrosing steatohepatitis in mice

To confirm the direct role of BMMs on fibrosing steatohepatitis, we performed adoptive transfer of BMMs (10^6 cells/week) into C57BL/6J mice by tail vein injection, and then fed with MCD diet for 5 weeks (Figure 4A). Adaptive transfer of BMMs to these mice resulted in increased lipid accumulation, inflammatory cell infiltration (Figure 4B), elevated serum ALT (Figure 4B), and enhanced collagen deposition (Figure 4C) and α-SMA protein expression (Figure 4D). Collectively, these results indicate that adoptive transfer of BMMs to MCD-fed mice aggravated fibrosing steatohepatitis in mice.

Macrophage conditional medium promotes the activation and proliferation of HSCs

To investigate the effect of macrophages on the activation of HSCs, macrophage conditioned medium were co-cultured with mouse primary HSCs, human HSC cell line (LX-2) and rat HSC cell line (HSC-T6) respectively (Figure 5A). Freshly isolated HSCs retain their quiescent phenotype with distinct stellate morphology (Figure 5B). Compared to the primary HSCs culture in control medium, HSCs cultured in macrophage conditioned medium from primary mouse macrophage were more frequently and quickly activated with typical activated morphology of a large, spread out, flattened polygonal shape at day 3, 5, and 7 (Figure 5B). The activation of HSCs was confirmed by significantly increased α-SMA and collagen I expression at day 3 and day 7 (Figure 5B). Moreover, macrophage-conditioned medium from the human macrophage cell line THP1 promoted the activation of human HSCs LX2, and macrophage-conditioned medium from primary rat macrophages promoted the activation of rat HSC-T6 cells, as indicated by increased protein levels of α-SMA and genes related to fibrogenesis, including for collagen I, TGFβ1 and Smad2 as well as ER stress markers GRP78, IRE1α, and PDI (Figure 5C). We further evaluated the effect of macrophages on HSC cell proliferation

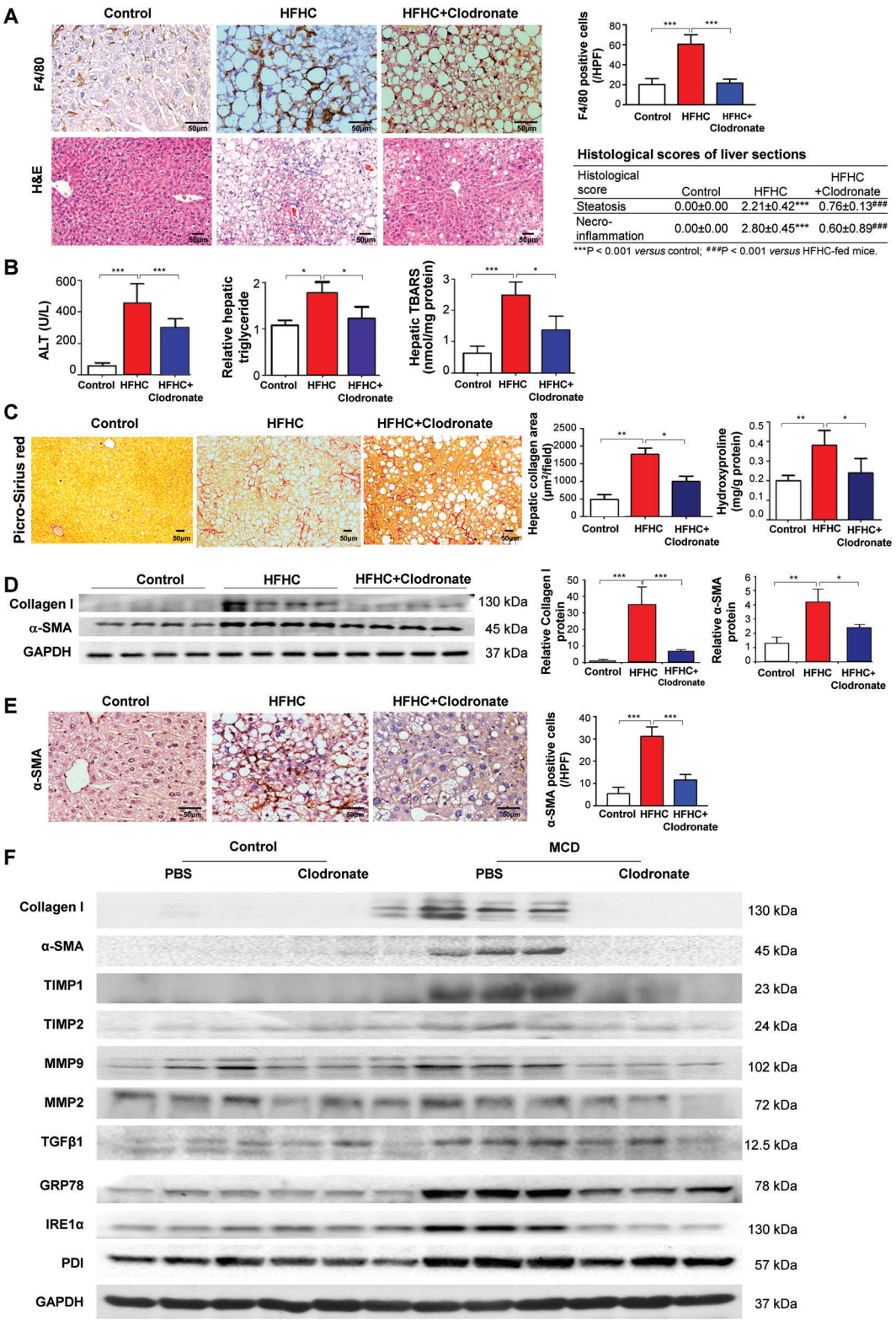

Figure 3. Macrophage depletion prevented high fat diet-induced fibrosing steatohepatitis in *foz/foz* mice. (A) Representative immunohistochemistry for F4/80 and H&E stained images of liver tissues from 12 weeks HFHC diet-fed *foz/foz* mice depleted of macrophages by clodronate treatment. Histological steatosis and necro-inflammation was scored in liver tissues by H&E staining. (B) Serum ALT, total hepatic lipoperoxide, and liver triglyceride content were determined. (C) Representative images of collagen fiber in liver tissues from 12 weeks HFHC diet-fed *foz/foz* mice and depleted by clodronate treatment. The amount of collagen protein was determined by Picro-Sirius Red staining and Hydroxyproline assay. (D) Collagen and α-SMA protein in liver tissues were determined by western blotting in tissues from12 weeks HFHC diet-fed *foz/foz* mice depleted of macrophages by clodronate treatment. (E) Immunohistochemistry analysis of α-SMA protein levels in HFHC diet-fed *foz/foz* mice. The number of α-SMA positive cells per high-power field was calculated. (F) Expression of hepatic proteins involved in collagen production (collagen I, TGFβ1), HSC activation (α-SMA), matrix degradation (TIMP1, TIMP2, MMP2, MMP9), and ER stress (GRP 78, IRE1α, PDI) in tissues from 8-week MCD-fed C57BL/6J mice depleted of macrophages by clodronate treatment, as determined by western blotting. $n = 5–8$/group. $^{*}P < 0.05$, $^{**}P < 0.01$, $^{***}P < 0.001$.

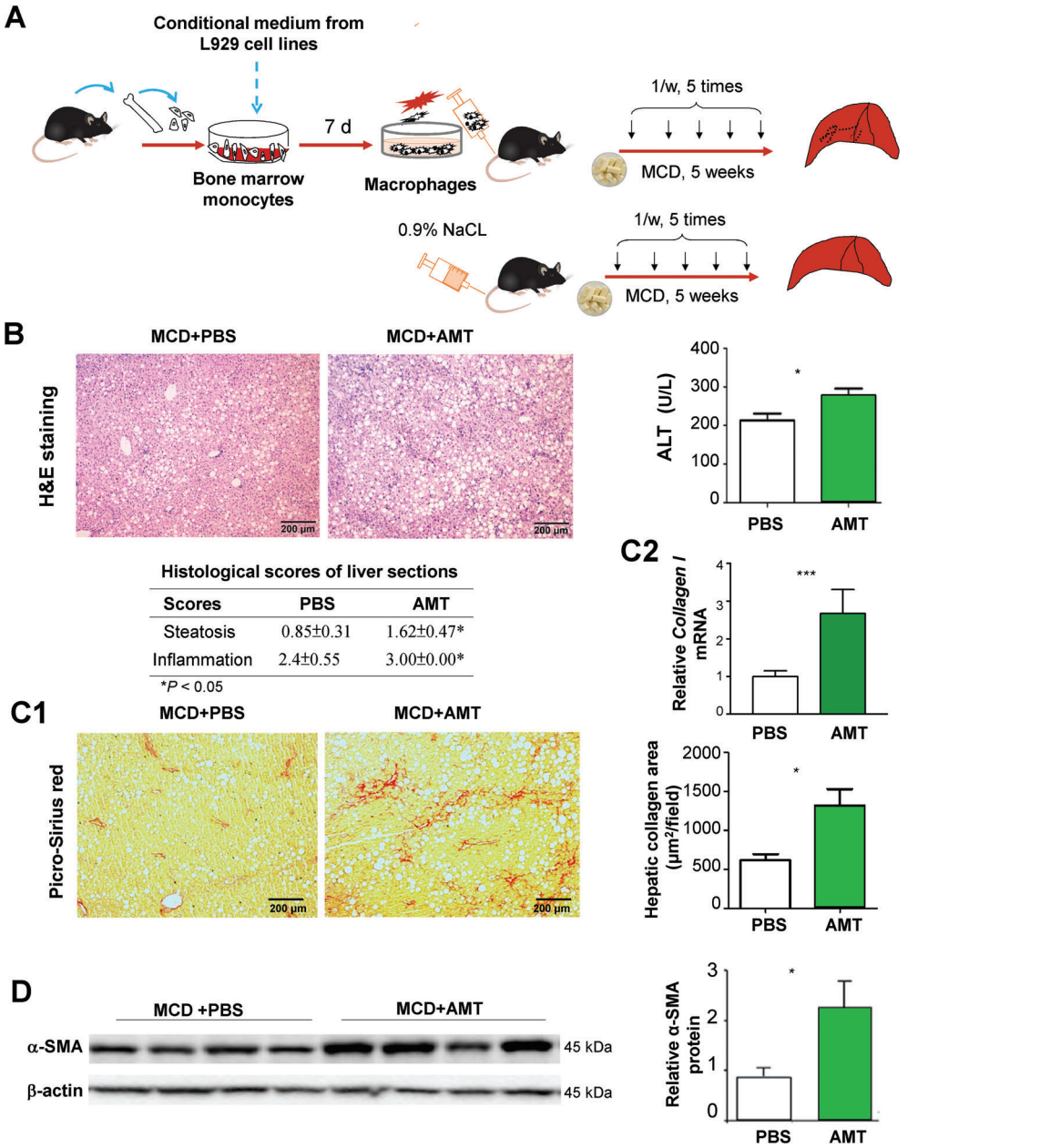

Figure 4. Adoptive transfer of BMMs aggravated fibrosing steatohepatitis in mice. (A) Schematic diagram of adoptive transfer of BMMs to MCD-fed C57BL/6J mice. Bone marrow cells were isolated from the femur and tibia of 8-week-old male C57BL/6J mice and stimulated by the cultured medium from L929 fibroblast cells, C57BL/6J-recipient mice were injected in the tail vein with BMMs then fed with MCD diet for 5 weeks. (B) Representative H&E staining images of liver tissues and serum ALT levels from MCD-fed C57BL/6J mice after adoptive transfer of BMMs. Histological steatosis and necro-inflammation were scored. (C) Collagen deposition from liver tissue was analyzed by (C1) Picro-Sirius Red staining and (C2) for collagen I mRNA levels. (D) Western blotting analysis of α-SMA protein levels in MCD-fed mice with or without macrophage adoptive transfer. $n = 5–8$/group. $^{*}P < 0.05$, $^{***}P < 0.001$.

and apoptosis. Macrophage conditioned medium promoted the cell proliferation but inhibited apoptosis in HSC cell lines LX2 and HSC-T6 (Figure 5D,E).

The pro-fibrosis effect of BMMs is mediated through induction of *C3ar1*

Having identified that BMMs could promote fibrosing steatohepatitis both *in vitro* and *in vivo*, we then investigated the molecular mechanisms of its function using a cDNA expression PCR array to identify genes and pathways involved in BMMs-induced fibrosis. As shown in Figure 6A, 42 genes were dysregulated by macrophage depletion in mice treated with clodronate with improved fibrosing steatohepatitis compared to PBS-treated mice with severe fibrosing steatohepatitis. These genes were mainly enriched in fibrosis signaling pathways of cytokine-cytokine receptor interaction, chemokine signaling, toll-like receptor signaling, TGFβ signaling, and complement and coagulation cascades (Figure 6B). The downregulation of key pro-fibrosis factors *C3ar1*, C-X-C chemokine receptor (*Cxcr*)1 and Toll-like receptor (*Tlr*)9 was confirmed at the mRNA level by RT-qPCR in both MCD-fed C57BL/6J WT

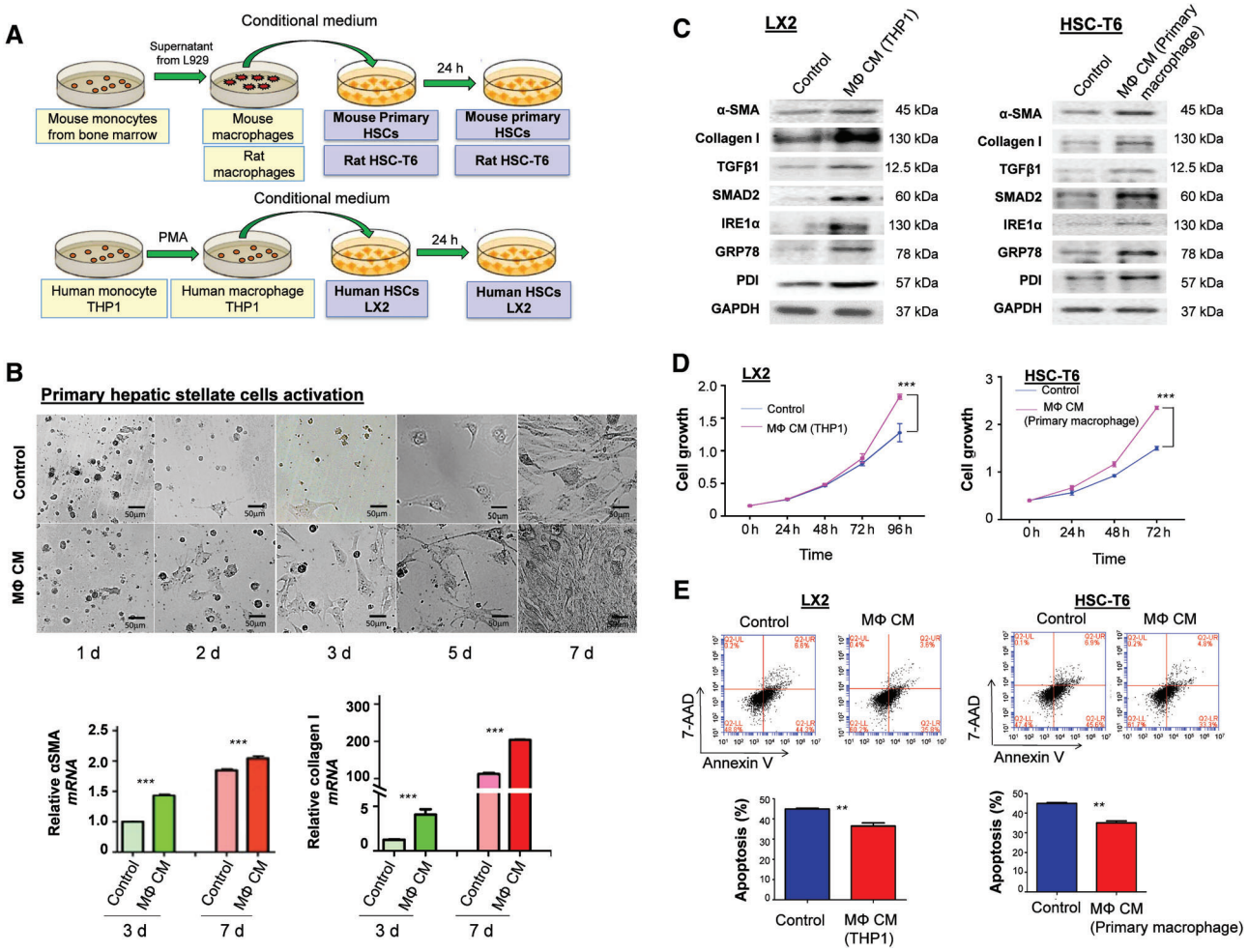

Figure 5. Macrophage conditional medium promoted the activation and proliferation of hepatic stellate cells. (A) Schematic diagram of bone marrow-derived macrophage's effect on activation of hepatic stellate cells *in vitro*. Human HSC cell line (LX-2), rat HSC cell line (HSC-T6) and mouse primary HSCs was cultured with 30% conditioned medium (CM) from PMA-stimulated human macrophages (THP1), L929 cell supernatant-stimulated mouse primary macrophages or rat primary macrophages, respectively. (B) Morphological characteristic of freshly isolated mouse primary HSCs at distinct times with or without macrophage-conditioned medium, also shown α-SMA and collagen mRNA expression. (C) The molecular mechanism of macrophage-conditioned medium promoting the activation of HSCs *in vitro*. Hepatic fibrosis related protein biomarkers of Collagen I, α-SMA, TGFβ1, Smad2 were determined in LX2 and HSC-T6 cell lines by western blotting, and of ER stress markers GRP78, IRE1α, and PDI. (D) The effect of macrophage-conditioned medium on LX2 and HSC-T6 cell proliferation and (E) apoptosis *in vitro*. Experiments were performed in triplicate and repeated three times. $^{**}P < 0.01$, $^{***}P < 0.001$.

mice and HFHC-fed *foz/foz* mice with macrophage depletion (Figure 6C). The decreased protein levels of the pro-inflammatory factors in liver tissues were verified by cytokine profiling assay in MCD-fed transgenic *LysM-Cre*/DTR mice with macrophage ablation (see supplementary material, Figure S3A). We found that macrophage depletion by DTox treatment significantly reduced the protein levels of TNFα ($p < 0.05$), IL-1β ($p < 0.01$), IL-1α ($p < 0.05$), and CCL3 ($p < 0.05$) (see supplementary material, Figure S3B) in the liver tissues of MCD-fed lysM-Cre/DTR mice compared to MCD-fed control mice.

Among the dysregulated genes, *C3ar1* was the most significantly downregulated gene by macrophage depletion (Figure 6A). We thus test the importance of *C3ar1* in liver fibrosis using *C3ar1*$^{-/-}$ mice. As shown in Figure 6D, *C3ar1*$^{-/-}$ mice fed MCD for 8 weeks only showed minor fibrosis with occasionally collagen, compared to the WT mice fed the same diet with pronounced fibrosis (Figure 6D). Concomitantly, α-SMA-positive cells (by IHC staining) were significantly fewer in *C3ar1*$^{-/-}$ mice compared to WT mice fed MCD (Figure 6D); protein expression of collagen I and α-SMA was reduced in *C3ar1*$^{-/-}$ mice than WT mice by Western blotting (Figure 6E). Collectively, these findings suggested that the effect of macrophage in promoting fibrosing steatohepatitis was at least in part by inducing hepatic C3ar1 (Figure 6F).

Discussion

In this study, we found significant increases in macrophage infiltration in fibrosing steatohepatitis of rodent and human liver. Macrophages have been reported to be implicated in inflammatory processes and in the development of various diseases [3].

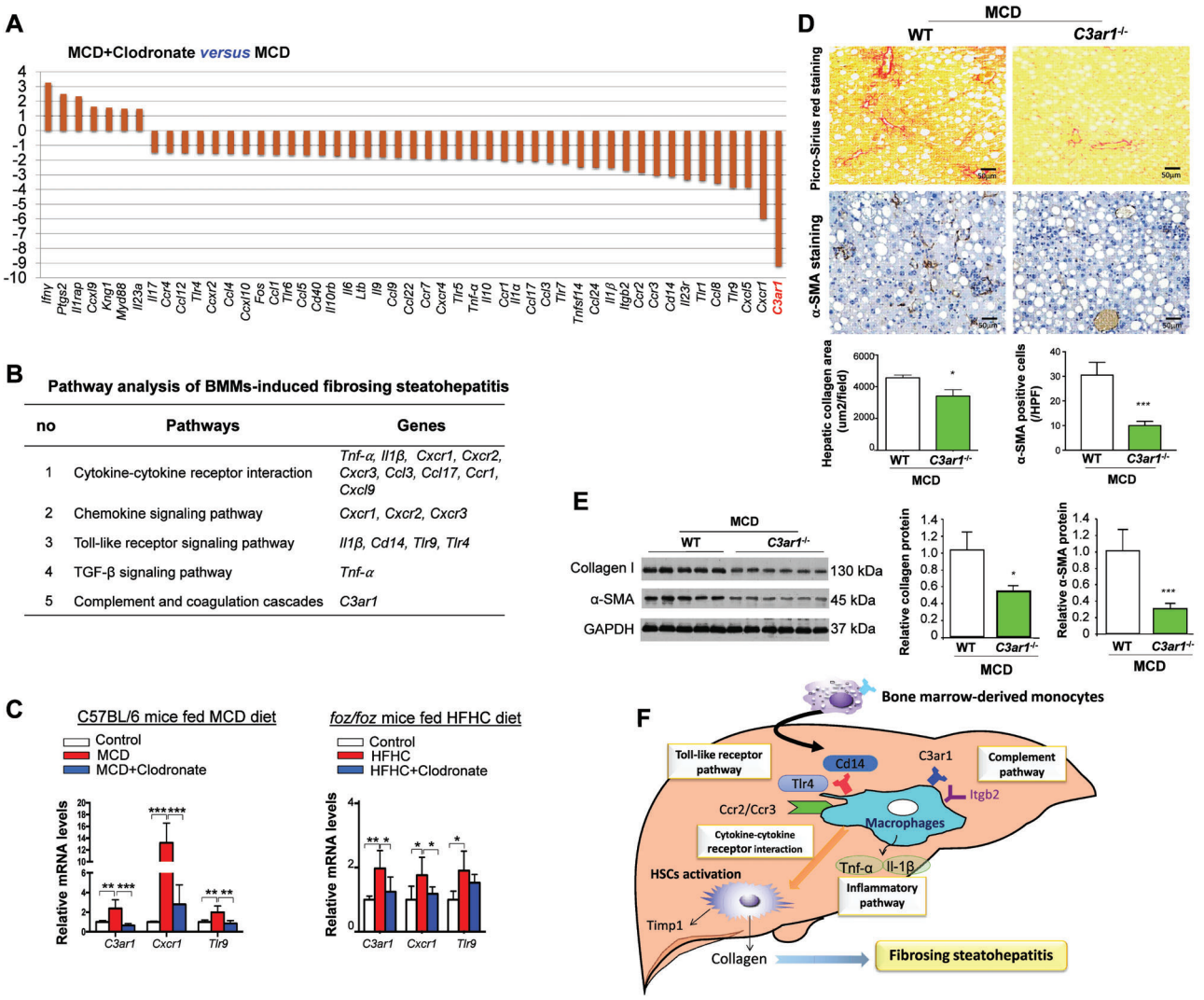

Figure 6. The pro-fibrosis effect of BMM is mediated through *C3ar1*. (A) The downstream effectors of BMM-induced fibrosing steatohepatitis were identified by cDNA expression PCR array. (B) The main signal pathways analysis of BMM induced fibrosing steatohepatitis. (C) The key pro-fibrosis factors including *C3ar1*, *Cxcr1*, and *Tlr9* mRNA expression were confirmed by qRT-PCR in both MCD-fed C57BL/6 WT mice and HFHC-fed *foz/foz* mice models. Values are mean ± SD ($n = 5$/group). *$p < 0.05$, **$p < 0.01$. (D) Representative Picro-Sirus Red and immunohistochemical staining for α-SMA of liver sections from C57BL/6J WT and *C3ar1*$^{-/-}$ mice fed MCD diet for 8 weeks. Collagen deposition from liver tissue was quantified by scanning Picro-Sirius Red density. The number of α-SMA positive cells/high-power field was counted. (E) Hepatic protein expression of collagen I and α-SMA as shown by western blotting. (F) Schematic diagram for the mechanisms of BMMs in the promotion of fibrosing steatohepatitis. Chemokine signaling pathway, toll-like receptor signaling pathway, cytokine-cytokine interaction and complement signaling pathway (*C3ar1*) was revealed to mediate HSC activation in the pathogenesis of fibrosing steatohepatitis. $n = 5–8$/group. *$P < 0.05$, **$P < 0.01$, ***$P < 0.001$.

In NAFLD progression, the increased abundance of portal macrophages was the earliest change in simple steatosis patients before the increased expression of pro-inflammatory cytokines seen in NASH patients [14]. Moreover, pro-inflammatory macrophages were identified as the predominant subset in pediatric NAFLD patients [15]. Macrophage infiltration was observed to coincide with increased accumulation of hepatic collagen and activation of HSCs. These results suggested that macrophages may play a role in the evolution of fibrosing steatohepatitis and their enhanced infiltration is associated with activation of HSCs. Macrophages in the liver do have multiple origins. Previous study revealed that hepatic macrophages can arise either from bone marrow monocyte-derived macrophages, BMMs, which are recruited to the injured liver via chemokine signals, or from self-renewing Kupffer cells [16]. In the uninjured liver and steady-state conditions, Kupffer cells are predominant and BMMs only a minor population [17]. Kupffer cells are the resident hepatic macrophages and comprise ~5% of liver cells. In the early stage of NASH, Kupffer cells become fat-loaded, recruit lymphocytes [18], and secret pro-inflammatory cytokines (IL-1β), thereby promoting steatohepatitis. Reduced liver injury, steatosis, and proinflammatory monocyte infiltration were reported upon depletion of Kupffer cells in MCD-induced steatohepatitis [19]. On the other hand, fibrogenic growth factors (TGFβ) secreted by Kupffer cells could promote HSC activation, leading to fibrosis development [20]. The infiltrating

Ly-6C$^+$ monocyte-derived macrophages are linked to chronic inflammation and fibrogenesis [16]. In this connection, we characterized the predominant origin of macrophages in hepatic fibrosing steatohepatitis using BMT from GFP$^+$ mice. Massive infiltration of BMMs was observed in the liver of fibrosing steatohepatitis (Figure 1). Mouse models also revealed that LY6C^{hi} expressing monocyte-derived macrophages are the predominant population accumulated in the fibrotic liver, suggesting that infiltrating BMMs exert major functions in the progression of fibrosing steatohepatitis.

If macrophages play a key part in fibrosing steatohepatitis, it would be important to investigate the effect of their depletion on the severity of liver fibrosis. To test this, hepatic macrophages were depleted by liposomal clodronate; a liposome-mediated macrophage suicide approach, based on the liposome-mediated internalization of the small hydrophilic molecule clodronate by macrophages. At a certain intracellular clodronate concentration, the macrophages are eliminated by apoptosis. We found that depletion of BMMs by liposomal clodronate during MCD-induced liver injury resulted in significantly attenuated liver fibrosis, concomitant with less accumulation of hepatic lipid, and less inflammation in C57BL/6J mice fed MCD (Figure 2). These results are congruent with reports that monocytes/macrophages blockade (by CCL2 or CCR2 inhibitors) during the early phase of acute liver injury is protective in C57BL/6J mice [21]. However, we found depletion of macrophages during the recovery phase aggravated fibrosing steatohepatitis (Figure S1). In line with our findings, other studies reported that macrophage depletion leads to a failure of liver regeneration [22]. Macrophages promote extracellular matrix accumulation during ongoing liver injury but enhanced matrix degradation during recovery [4]. Thus, macrophages play diverse function in homeostasis, disease progression, and regression from injury. They exert critical functions in the initiation of inflammation and the induction of liver fibrosis during chronic liver injury [23]. On the other hand, macrophages play key regulatory roles in the injured tissue regeneration and fibrosis regression through extracellular matrix degradation [5]. Moreover, macrophages are critical for hepatic immunity and removal of gut-derived pathogens [24]. Taken together, the function of macrophages in liver fibrosis is distinct during different stages of tissue repair.

Understanding of the effect of BMMs depletion during injury, to repress fibrosing steatohepatitis, was refined in *foz/foz* mice (Figure 3). We showed that expression of α-SMA, collagen I, TIMP-1, TIMP2, MMP9, MMP2, and TGFβ1 was upregulated in fibrosing steatohepatitis in mice. These genes are mainly expressed by HSCs during fibrogenesis as critical pro-fibrosing factors [25]. Depletion of BMMs resulted in significant downregulation of these pro-fibrosing factors, which is more likely the result of reduced activation of HSCs (Figure 3). Moreover, ER stress has been implicated in the development of fibrotic process [26]. We found that the ER stress was induced in fibrosing steatohepatitis with enhanced protein levels of ER stress markers GRP78, IRE1α, and PDI, whilst these markers were markedly blunted by depletion of BMMs in keeping with the attenuated fibrosing steatohepatitis, suggesting the involvement of ER stress in BMMs-induced fibrosing steatohepatitis. Collectively, these results demonstrated for the first time that targeted depletion of BMMs during liver injury is potentially a promising method for the treatment of fibrosing steatohepatitis. Because hepatic accumulation of BMMs is a feature of experimental fibrosing steatohepatitis, an adoptive transfer approach was used to directly assess the potential of BMMs to induce liver injury of fibrosing steatohepatitis. Indeed, adoptive transfer of monocytes from bone marrow into MCD-fed mice led to a significantly pronounced fibrosing steatohepatitis, evidenced by enhanced collagen deposition, α-SMA activation, increased lipid accumulation, and inflammatory infiltration. These results provided further direct evidence that macrophages can induce fibrosing steatohepatitis.

The molecular mechanisms by which macrophage exerts its pro-fibrosis function in steatohepatitis were evaluated. We demonstrated that macrophage-conditioned medium could induce the activation and proliferation of HSCs cells *in vitro* and suppress their apoptosis, concomitant with increased protein levels of pro-fibrosis markers TGFβ1, collagen I, and α-SMA (Figure 5). These results further confirmed the findings from *in vivo* mouse models, and collectively suggested that macrophage promotes fibrosing steatohepatitis by directly inducing the activation of HSCs and the consequent production of pro-fibrotic factors.

Having shown that macrophage is a crucial mediator in promoting fibrosing steatohepatitis through inducing the activation of HSCs, we looked for the critical effector of macrophage participating in its function. Using cDNA expression array, macrophage dysregulated proinflammatory factors, cytokine/chemokines, and their enriched signaling pathways including cytokine signaling, chemokine signaling, and TGFβ signaling were demonstrated. This information highlights the potential mechanism of macrophage in inducing these pathways to contributing fibrosing steatohepatitis. Among the dysregulated factors, C3ar1 was identified as one of the predominantly downregulated proteins by BMMs depletion (Figure 6). C3ar1 is a G protein-coupled receptor protein involved in the complement system and can induce the production of IL-1β and TGFβ [27]. It has been reported that an activated complement system releases the anaphylatoxin C3a, which binds to C3ar1 located on the membranes of macrophages, thereby activating macrophages [28]. We found that *C3ar1* knockout mice showed significantly less severe fibrosing steatohepatitis, along with reduced HSC activation compare to the wildtype littermates. Therefore, C3ar1 is an important effector in macrophage induced fibrosing steatohepatitis.

In conclusion, hepatic macrophages recruited from the bone marrow promote the progression of fibrosing steatohepatitis during liver injury through HSCs activation and proliferation, ER stress, and activation of complement system *C3ar1*. However, macrophages exhibit anti-fibrotic effect during recovery from liver injury. Targeting macrophages to reduce their pro-fibrotic activity and improve their anti-fibrotic activity is a potential promising approach for the treatment of fibrosing steatohepatitis. This paves the way for future research on macrophage-targeted therapy.

Acknowledgements

The project was supported by the RGC-GRF Hong Kong (14106415, 14111216, 14163817); RGC-CRF Hong Kong (C4041-17GF; C7026-18G; C7065-18G); CUHK direct grant for research; Vice-Chancellor's Discretionary Fund CUHK. The human liver specimens were provided by Prof. Vincent WS Wong in the Prince of Wales Hospital, the Chinese University of Hong Kong, and Prof. Kwan Man in the Queen Mary Hospital, University of Hong Kong, Hong Kong.

Author contributions statement

JH and XZ were involved in study design, conducted the experiments, and drafted the paper. JKL, KF, HCHL, WX, and ESC performed the experiments. JKL revised the paper. HL commented on the study. JY designed, supervised the study and wrote the paper.

References

1. Rinella ME. Nonalcoholic fatty liver disease: a systematic review. *JAMA* 2015; **313:** 2263–2273.
2. Schuppan D, Kim YO. Evolving therapies for liver fibrosis. *J Clin Invest* 2013; **123:** 1887–1901.
3. Pellicoro A, Ramachandran P, Iredale JP, *et al.* Liver fibrosis and repair: immune regulation of wound healing in a solid organ. *Nat Rev Immunol* 2014; **14:** 181–194.
4. Duffield JS, Forbes SJ, Constandinou CM, *et al.* Selective depletion of macrophages reveals distinct, opposing roles during liver injury and repair. *J Clin Invest* 2005; **115:** 56–65.
5. Wynn TA, Vannella KM. Macrophages in tissue repair, regeneration, and fibrosis. *Immunity* 2016; **44:** 450–462.
6. Zhang X, Han J, Man K, *et al.* CXC chemokine receptor 3 promotes steatohepatitis in mice through mediating inflammatory cytokines, macrophages and autophagy. *J Hepatol* 2016; **64:** 160–170.
7. Van Rooyen DM, Larter CZ, Haigh WG, *et al.* Hepatic free cholesterol accumulates in obese, diabetic mice and causes nonalcoholic steatohepatitis. *Gastroenterology* 2011; **141:** 1393–1403, 1403.e1-5.
8. Shen J, Chan HL, Wong GL, *et al.* Non-invasive diagnosis of non-alcoholic steatohepatitis by combined serum biomarkers. *J Hepatol* 2012; **56:** 1363–1370.
9. European Association for the Study of the Liver. EASL-EASD-EASO Clinical Practice Guidelines for the management of non-alcoholic fatty liver disease. *J Hepatol* 2016; **64:** 1388–1402.
10. Chalasani N, Younossi Z, Lavine JE, *et al.* The diagnosis and management of nonalcoholic fatty liver disease: practice guidance from the American Association for the Study of Liver Diseases. *Hepatology* 2018; **67:** 328–357.
11. Pradere JP, Kluwe J, De Minicis S, *et al.* Hepatic macrophages but not dendritic cells contribute to liver fibrosis by promoting the survival of activated hepatic stellate cells in mice. *Hepatology* 2013; **58:** 1461–1473.
12. Baeck C, Wei X, Bartneck M, *et al.* Pharmacological inhibition of the chemokine C-C motif chemokine ligand 2 (monocyte chemoattractant protein 1) accelerates liver fibrosis regression by suppressing Ly-6C(+) macrophage infiltration in mice. *Hepatology* 2014; **59:** 1060–1072.
13. Ginhoux F, Tacke F, Angeli V, *et al.* Langerhans cells arise from monocytes in vivo. *Nat Immunol* 2006; **7:** 265–273.
14. Gadd VL, Skoien R, Powell EE, *et al.* The portal inflammatory infiltrate and ductular reaction in human nonalcoholic fatty liver disease. *Hepatology* 2014; **59:** 1393–1405.
15. Carpino G, Nobili V, Renzi A, *et al.* Macrophage activation in pediatric nonalcoholic fatty liver disease (NAFLD) correlates with hepatic progenitor cell response via Wnt3a pathway. *PLoS One* 2016; **11:** e0157246.
16. Ramachandran P, Pellicoro A, Vernon MA, *et al.* Differential Ly-6C expression identifies the recruited macrophage phenotype, which orchestrates the regression of murine liver fibrosis. *Proc Natl Acad Sci U S A* 2012; **109:** E3186–E3195.
17. Beattie L, Sawtell A, Mann J, *et al.* Bone marrow-derived and resident liver macrophages display unique transcriptomic signatures but similar biological functions. *J Hepatol* 2016; **65:** 758–768.
18. Leroux A, Ferrere G, Godie V, *et al.* Toxic lipids stored by Kupffer cells correlates with their pro-inflammatory phenotype at an early stage of steatohepatitis. *J Hepatol* 2012; **57:** 141–149.
19. Tosello-Trampont AC, Landes SG, Nguyen V, *et al.* Kuppfer cells trigger nonalcoholic steatohepatitis development in diet-induced mouse model through tumor necrosis factor-alpha production. *J Biol Chem* 2012; **287:** 40161–40172.
20. Lee UE, Friedman SL. Mechanisms of hepatic fibrogenesis. *Best Pract Res Clin Gastroenterol* 2011; **25:** 195–206.
21. Mossanen JC, Krenkel O, Ergen C, *et al.* Chemokine (C-C motif) receptor 2-positive monocytes aggravate the early phase of acetaminophen-induced acute liver injury. *Hepatology* 2016; **64:** 1667–1682.
22. Ju C, Reilly TP, Bourdi M, *et al.* Protective role of Kupffer cells in acetaminophen-induced hepatic injury in mice. *Chem Res Toxicol* 2002; **15:** 1504–1513.
23. Tacke F, Zimmermann HW. Macrophage heterogeneity in liver injury and fibrosis. *J Hepatol* 2014; **60:** 1090–1096.
24. Gao B, Jeong WI, Tian Z. Liver: an organ with predominant innate immunity. *Hepatology* 2008; **47:** 729–736.
25. Friedman SL. Molecular regulation of hepatic fibrosis, an integrated cellular response to tissue injury. *J Biol Chem* 2000; **275:** 2247–2250.
26. Heindryckx F, Binet F, Ponticos M, *et al.* Endoplasmic reticulum stress enhances fibrosis through IRE1alpha-mediated degradation of miR-150 and XBP-1 splicing. *EMBO Mol Med* 2016; **8:** 729–744.
27. Li L, Yin Q, Tang X, *et al.* C3a receptor antagonist ameliorates inflammatory and fibrotic signals in type 2 diabetic nephropathy

by suppressing the activation of TGF-beta/smad3 and IKBalpha pathway. *PLoS One* 2014; **9:** e113639.

28. Zheng ZY, Weng SY, Yu Y. Signal molecule-mediated hepatic cell communication during liver regeneration. *World J Gastroenterol* 2009; **15:** 5776–5783.

*29. Li C, Kong Y, Wang H, *et al.* Homing of bone marrow mesenchymal stem cells mediated by sphingosine 1-phosphate contributes to liver fibrosis. *J Hepatol* 2009; **50:** 1174–1183.

*30. Kleiner DE, Brunt EM, Van Natta M, *et al.* Design and validation of a histological scoring system for nonalcoholic fatty liver disease. *Hepatology* 2005; **41:** 1313–1321.

*31. Liang W, Menke AL, Driessen A, *et al.* Establishment of a general NAFLD scoring system for rodent models and comparison to human liver pathology. *PLoS One* 2014; **9:** e115922.

*32. Zhang X, Shen J, Man K, *et al.* CXCL10 plays a key role as an inflammatory mediator and a non-invasive biomarker of non-alcoholic steatohepatitis. *J Hepatol* 2014; **61:** 1365–1375.

*33. Mederacke I, Dapito DH, Affo S, *et al.* High-yield and high-purity isolation of hepatic stellate cells from normal and fibrotic mouse livers. *Nat Protoc* 2015; **10:** 305–315.

*Cited only in supplementary materials.

SUPPLEMENTARY MATERIAL ONLINE

Supplementary materials and methods

Appendix 1. RT2 profiler PCR array gene expression analysis report

Figure S1. Macrophage depletion during recovery phase aggravated fibrosing steatohepatitis

Figure S2. Semi-quantitative analysis of western blotting bands for hepatic collagen I, TGFβ1, α-SMA, TIMP1, TIMP2, MMP2, MMP9, GRP 78, IRE1α, and PDI in C57BL/6 mice treated with clodronate or control (PBS) and fed with control or MCD diet

Figure S3. Macrophage depletion by Dtox treatment decreased the protein levels of TNF-α, IL-1β, IL-1α and CCL2 in the LysM-Cre transgenic mice

Table S1. Clinical characteristics of the patient populations

Table S2. Additional patient information

Table S3. Sequence of primers used for qPCR

Table S4. CT values for beta-actin mRNA in RT-qPCR